Master's Thesis

Reservoir computing based on explosive synchronization and quenched chaos

Jaesung Choi

Department of Mathematical Sciences

Graduate School of UNIST

2019

Reservoir computing based on explosive synchronization and quenched chaos

Jaesung Choi

Department of Mathematical Sciences
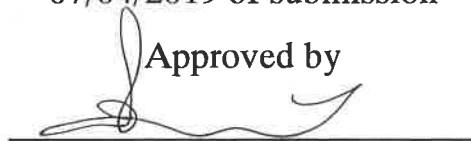
Graduate School of UNIST

UNIST

Reservoir computing based on explosive

synchronization and quenched chaos

A dissertation

submitted to the Graduate School of UNIST

in partial fulfillment of the

requirements for the degree of

Master of Science

Jaesung Choi

07/04/2019 of submission

Approved by
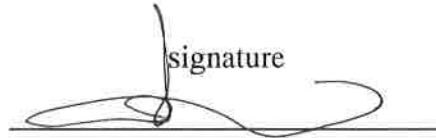
_____

Advisor

Pilwon Kim

Reservoir computing based on explosive

synchronization and quenched chaos

Jaesung Choi

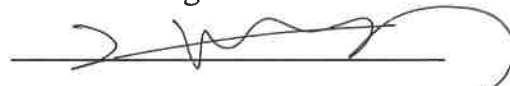This certifies that the dissertation of Jaesung Choi is approved.

07/04/2019 of submission

signature

Advisor: Prof. Pilwon Kim

signature

Prof. Bongsoo Jang: Thesis Committee Member #1

signature

Prof. Yunho Kim: Thesis Committee Member #2

Abstract

Synchronous oscillations in neuronal ensembles have been proposed to provide a neural basis for the information processes in the brain. In this work, we present a reservoir computing(RC), a highly efficient bio-inspired architecture, based on oscillator synchronization in a critical regime. The algorithm uses the high-dimensional transient dynamics perturbed by an input and translates it into proper output stream. One of the benefits of adopting coupled phase oscillators as neuromorphic elements is that the synchrony among oscillators can be finely tuned at artificial state. Especially near a critical state, the marginally synchronized oscillators operate with high efficiency and maintain better computing performances. We also show that explosive synchronization that is induced from specific neuronal connectivity produces more improved and stable outputs. This work provides a systematic way to encode computing in a large size coupled oscillator, which may be useful in designing neuromorphic devices.

Furthermore we develop RC based on "explosive death" of chaos. The proposed reservoir utilizes transient dynamics of coupled chaotic oscillators in a critical regime where sudden amplitude death occurs. Explosive death not only brings the system a large criticality which provides a variety of orbits for computing, but also stabilizes them which otherwise diverge soon in chaotic units. The proposed framework shows better results in tasks for signal reconstructions than RC based on explosive synchronization of regular phase oscillators. We also show that the information capacity of the reservoirs at a critical point can be used as a predictive measure for computational capability of a reservoir.

Contents

I Introduction

Recently, reservoir computing has emerged as a promising computational framework for utilizing a dynamical system for computation. While an input stream perturbs the transient intrinsic dynamics of a medium(the "reservoir"), a readout layer is trained to extract features out of such perturbations to reconstruct a target output. Due to its complex high-dimensional dynamics, the reservoir serves as a vast repertoire of nonlinear transformations that can be exploited by the readout. The major advantage of reservoir computing is their simplicity in training process compared to other neural networks. Another advantage is their universality in that they can be realized using physical systems, substrates, and devices. [1]

There is the hypothesis that a system can exhibit maximal computational power at a phase transition between ordered and chaotic behavioral regimes [2,3]. It has been observed that the brain operates near a critical state in order to adapt to a great variety of inputs and maximize information capacity [4–6]. Perturbations occurring in a critical regime neither spread nor die out too quickly, providing the most flexibility to the system [7,8]. This concept of "computation at the edge of chaos" may also have an implication to material computation, whereby a material has the most exploitable properties [9]. More extensive review on this subject can be found in [10].

In RC, designing a reservoir which has a "large criticality" is important to perform complex tasks. In case of a reservoir based on continuous dynamical systems, one can create criticality by tuning intrinsic parameters so that the reservoir operates at a bifurcation point across which the dimension of the attractor abruptly declines. A system of coupled oscillator exhibits a first order transition from incoherent state to synchronized state that occurs under a specific relation between the coupling strength and connectivity, which is called explosive synchronization. In the second section, we show that a reservoir of coupled Kuramoto oscillators performs excellent computations in a critical regime near explosive synchronization.

Amplitude death is another way to create a criticality in coupled oscillatory units. It indicates complete cessation of oscillations induced from change in intrinsic parameters of the system. The occurrence of AD has been found in the case of chemical reactions [11, 12], neuronal systems [13, 14] and coupled laser systems [15, 16]. Several underlying mechanisms for AD have been identified so far, including de-tuning of oscillators under strong coupling, conjugate coupling, dynamic coupling, and delay in coupling [17]. Recently, it has been reported that AD can occur abruptly in systems of coupled nonlinear oscillators [18–21]. This first-order transition to AD is called "explosive death".

There have been numerous researches on using chaotic systems for computation [22, 23], even in the context of RC [24–26]; Chaos computing takes advantage of an infinite number of orbits/patterns inherent in the attractor to be used for particular computational tasks. It also utilizes the sensitivity to initial conditions of chaotic systems to perform rapid switching between computational modes. However, chaos computing has a control problem to stabilize particular

orbit.

In the third section, we develop RC based on explosive death of chaos. We construct a chaotic based reservoir with a large criticality and identify the effect of chaotic properties. The proposed reservoir utilizes transient dynamics of a coupled chaotic oscillators in a critical regime where sudden amplitude death occurs. Explosive death not only brings the system a large criticality which provides a variety of orbits for computing, but also stabilizes them which otherwise diverge soon in chaotic units. Another goal of the study is to find a predictive measure for computational capability of a reservoir. So in the last section, we introduce the total capacity proposed in [27]. We compared proposed the tendency between capacity and errors for several tasks. And we checked that it can be a reliable measure for reservoir computing based on dynamical oscillators.

II Reservoir Computing based on Explosive Synchronization

2.1 Model : Kuramoto Oscillators

A. Reservoir of oscillatory networks

The reservoir of oscillatory networks uses a phase-locked state as the ground state for computations. Once perturbed by inputs, the deviation of the oscillators from the synchronized state is closely observed until they return to the original state. The basic idea underlying the oscillatory reservoir computing is that, if network is large enough, all the information necessary to construct proper computational results can be found in the transient trajectories aroused by inputs.

We consider a network of N oscillators, being the dynamics of each of them described by a phase $\theta_i(t) \in [0, 2\pi)$:

$$\theta_i' = \omega_i + \frac{\lambda_i}{k_i} \sum_{j=1}^{N} A_{ij} \sin(\theta_j - \theta_i), \quad i = 1, \cdots, N, \tag{1}$$

where ω_i is the natural frequency, $\lambda_i > 0$ is the coupling strength, and $k_i := \sum_{j=1}^{N} A_{ij}$ is the degree of the node i. Here A_{ij} is the entry of the adjacency matrix of the network which is equal to 1 if nodes i and j are connected, and zero if they are not. The classical Kuramoto model is defined on the complete graph with an identical coupling strength, that is, $\lambda_i = \lambda$ and $A_{ij} = 1$ for all i and j. It is commonly observed that a modest coupling strength $\lambda_i > \lambda_C$ in (1) drives the oscillators into a phase-locked state in which they maintain a frozen formation at the same frequency. For given network topology and frequency distribution, one usually is interested in assessment of the critical coupling strength λ_C at which a phase transition occurs from incoherency to a phase-locked state.

We can use a measure of synchrony to capture an appropriate coupling strength that leads to the phase-locked states. One measure of synchrony is the Kuramoto order parameter:

$$re^{i\theta} = \frac{1}{N} \sum_{j=1}^{N} e^{i\theta_j}.$$

The order parameter r achieves its maximum 1 when the phase of all oscillators are identical in complete phase synchronization. It becomes close to 0 when the phases are scattered around the circle in dynamical incoherence. The graph(black rectangles) in Figure 1(a) shows how the magnitude of the order parameter r rises with the coupling strength λ in the classical Kuramoto model. The order parameter attains non-zero value for couplings stronger than the critical value $\lambda_C \approx 1.6$, indicating the onset of synchronization.

Increasing the coupling strength in oscillator networks brings the individual frequencies of oscillators one by one to the average frequency of the system until full synchronization is achieved. Recently, in a certain type of oscillator networks [21, 28], discontinuous transitions from incoherent states to phase-locked states have been reported. In those systems, all the effective

frequencies persist right up to the synchronization transition and then they suddenly jump to the average frequency simultaneously at the critical point. This phenomenon, called explosive synchronization(ES), was proved to be originated from a positive correlation between the natural frequencies and the coupling strengths of oscillators [29]. More specifically, if the coupling strength is proportional to the natural frequency

$$\lambda_i = \lambda|\omega_i|, \quad \lambda > 0, \tag{2}$$

the phase dynamics in (1) induces explosive synchronization.

The explosive synchronization occurs with hysteresis: besides the forward transition from the incoherent state to the phase-locked states, there is also an abrupt desynchronization with decrease of the coupling strength, which does not overlap with the forward transition. However, we only focus on the forward bifurcation in neuromorphic computing, as we need to keep the system out of the hysteresis loop, avoiding the risk of permanent desynchrony. The plot(red circles) in Figure 1(a) shows that forward discontinuous phase transition occurs at a critical coupling strength $\lambda \approx 2.9$, making striking difference from the continuous phase transition at $\lambda \approx 1.6$.

In this work, we compare the two computing reservoirs based on the Kuramoto model (1) which use the different settings for the coupling strength and the network topology:

1) **Regular synchronization model(RS)**
   coupling strength: $\lambda_i = \lambda > 0$,
   network topology: $A_{ij} = 1$ if $i \neq j$, otherwise 0.
2) **Explosive synchronization model(ES)**
   coupling strength: $\lambda_i = \lambda|\omega_i| \ \lambda > 0$,
   network topology: a Erdős-Rényi graph with $1 \leq \langle k_i \rangle < N$

RS is nothing but the classical Kuramoto model. ES adopts a Erdős-Rényi graph, which is chosen uniformly at random from the collection of all graphs which have N nodes with a specific mean degree $\langle k_i \rangle$. From here on, we will use networks that consist of $N = 500$ oscillators for both models. The natural frequencies ω_i of oscillators are assumed to follow the normal distribution $N(0, 1)$.

B. Choice of coupling strength

In Kuramoto-based models, a higher coupling strength makes the oscillators synchronized in a tighter phase-locked state. If the synchronization is overly persistent, the transient dynamics induced from the inputs vanish so quickly that it cannot properly handle lengthy computations. On the other hand, under a weak coupling strength, the system may fail to erase the past information which is no more necessary and interferes the current computation as noise. Moreover,

the oscillators may not be able to recover the ground state even after the computation is carried out.

For balanced computations, it is reasonable to set the coupling strength at which the phase of the oscillators are marginally locked and can react rapidly to external stimuli. The Kuramoto order parameter r can be used as an indicator for a critical value of the coupling strength λ. For ES illustrated in Figure 1(a), one may fix the value of λ at near 2.9 where r drops quickly in the backward direction. However, for RS, the phase transition in r gradually arises with λ and therefore does not provide a sharp criterion. Moreover, it is not the edge of chaos but the edge of order where the efficient computations occur, in that the system should maintain synchronization as a ground state. Since the conventional Kuramoto order parameter r only yields the continuous phase transition, it is not a good indicator for computational capacity.

In order to overcome this drawback of r, we introduce the variance order parameter r_{var} as

$$r_{\mathrm{var}} = \frac{1}{N} \sum_{j=1}^{N} \exp(-c \, \mathrm{var}_j), \quad c > 0 \tag{3}$$

where var_j is the temporal variance of the frequency $\theta'_j(t)$. This is a measure for desynchrony that sensitively shows a degree of deviation of oscillators from a steady frequency. For reliable computations, the temporal variance of the frequency should be kept low in the ground state. Note that, for each oscillator, the temporal variance of the frequency becomes 0 if oscillators are in a phase-locked state, keeping their common frequency steady. The variance order parameter indicates a critical point more clearly than the Kuramoto order parameter and is also easier to compute, since it is evaluated from temporal evolution of individual oscillators. The factor c stands for a sensitivity to deviation from the ground state. In case of ES, the acceptable range for c is $10^2 \leq c \leq 10^8$,, regardless of the network topology of coupled oscillators. A value of c smaller or larger than this range tends to fix r_{var} to 1 or 0, respectively, making it impractical as an order parameter.

Figure 1(b) plots r_{var} for the same formations of the oscillators dealt in 1(a). While r_{var} almost coincides with r for ES at the critical strength($\lambda \approx 3$), it clearly reveals a discontinuous phase transition for RS which is not observed in r. Although r_{var} does not explicitly show difference between explosive and nonexplosive synchronizations, it provides clear information on a level of the coupling strength for which oscillators are arranged for reliable computations. From here on, we will use the variance order parameter r_{var} to investigate the relation between the states of the system and its computing performances.

C. Readout and training

The oscillator networks are applied to supervised tasks to learn a model that produces a target output $v(t) = (v^1(t), \cdots, v^q(t)) \in \mathbb{R}^q$ from an input signal $u(t) = (u^1(t), \cdots, u^p(t)) \in \mathbb{R}^p$. In practice the dataset can be either discrete or continuous in time, and also can be multi dimensional signals, but this does not change the principles. We set p oscillators to the input
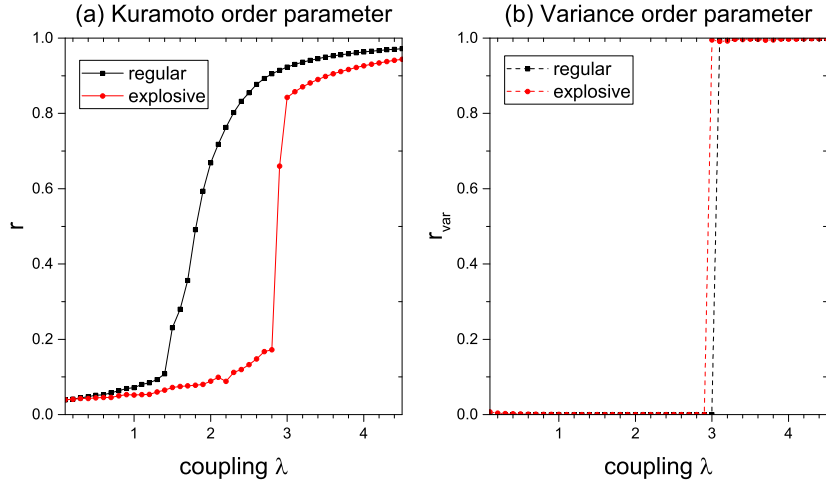
Figure 1: Kuramoto and variance order parameters according to the coupling strength: RS and ES use the complete network and a Erdős-Rényi graph with the mean degree $\langle k_i \rangle = 6$, respectively. In ES, only forward transitions are plotted. The parameter $c = 10^7$ is used for the variance order parameter.

nodes of the reservoir. The standard training starts with running the network until it reaches a phase locked state. Once oscillators are synchronized, we feed the network the input stream $u(t)$, by completely synchronizing p oscillators(input nodes) in the network with $u(t)$. That is, the way to deliver an input signal $u(t)$ to the reservoir is making the input nodes follow the same dynamics of $u(t)$ while it is given. All evolutionary activities of the oscillators are collected through the frequency values $\theta_i'(t)$ and mapped to the desired output by a output function $f_{\text{out}} = (f_{\text{out}}^1, \cdots, f_{\text{out}}^q) \in \mathbb{R}^q$.

In the readout process, it is better to use not only the past values of the nodes as well as the current ones, to exploit the rich dynamics of the chaotic reservoirs. Here we use a output function that takes past s sampled states of the system at discrete times $t - \Delta t, t - 2\Delta t, \cdots, t - s\Delta t$ and maps them to the desired output at time t. We define the output function $f_{\text{out}} = (f_{\text{out}}^1, \ldots, f_{\text{out}}^q) \in \mathbb{R}^q$ of $(s, \Delta t)$-type as

$$f_{\text{out}}^l(t) = \sum_{i=1}^N \sum_{j=1}^s w_{i,j}^l \theta_i'(t - (j-1)\Delta t), \quad l = 1, \cdots, q \qquad (4)$$

The weights $w_{i,j}^l$ are determined so that $f_{\text{out}}(t)$ matches $v(t)$ as close as possible, minimizing an error measure. For example, if the available output data is a time series of total length M, $v(t_1), v(t_2), \cdots, v(t_M)$, a typical mean-square error is

$$\frac{1}{M} \sum_{i=1}^M \|v(t_i) - f_{\text{out}}(t_i)\|^2. \qquad (5)$$

And relative mean-square error is

$$\frac{\sum_{i=1}^M \|v(t_i) - f_{\text{out}}(t_i)\|^2}{\sum_{i=1}^M \|v(t_i)\|^2}. \qquad (6)$$

6

Mean-square error and relative mean-square error are applied for section2 and 3, respectively.

2.2 Numerical Tests

In the following numerical examples to test the learning ability of the oscillator networks, we use the $(10, 0.1)$-type readout function: The output $f_{\text{out}}(t)$ at t is obtained from 10 previous sampled values of the oscillator frequencies $\theta_i'(t - 0.1), \cdots, \theta_i'(t - 1)$ through the equation (4).

We set up two tasks, filtering and forecasting, both of which require the presence of long-term memory for proper execution. Task 1 is to learn the scalar output

$$v(t) = \frac{1}{m} \sum_{k=1}^{m} \left(au(t - k) + bu(t - k)^2 + cu(t - k)^3 \right) \tag{7}$$

which is determined from the past m values of an input stream $u(t)$. Here a, b and c are some nonzero parameters. We use the input $u(t)$ generated from the Lorenz system which provides standard benchmark task for chaotic series handling [30]. Note that, if $m = 1$, the task is simply to implement a polynomial function of the current value of the input. The task becomes more challenging as m increases, requiring long-term memory to evaluate averaged values.

Task 2 is the time series prediction. Based on a previous input stream of $u(t)$, the network is required to predict m steps ahead, that is, the next m values, $u(t + 1), \cdots, u(t + m)$. This implies that the desired output vector $v(t) = (v^1(t), \cdots, v^m(t)) \in \mathbb{R}^m$ at time t satisfies $v^l(t) = u(t + k)$, $k = 0, \cdots, m - 1$. We take the input $u(t)$ from Mackey-Glass equation which is a chaotic time-delayed differential equation.

In each task, the continuous input signal $u(t)$ and the target signal $v(t)$ are generated for $t \in [0, 5000]$. The training process is applied to match $f_{\text{out}}(t)$ to y(t) over the first 4,000 discrete time steps, $t = 1, 2, \cdots, 4000$. That is, the readout weights w_{ij}^l in (4) are determined to minimize the averaged error (4) with respect to $M = 4000$. Then we measure the performance using the remaining part of the signal for $t \in (4000, 5000]$: the averaged error (5) between $f_{\text{out}}(t)$ to $v(t)$ is evaluated over 1,000 discrete sampled time steps.

A. Computing performance at the critical point

We first illustrate the computational performance of RS on complete networks. Figures 2 (a) and (b) respectively reports the averaged errors in task 1 and 2. We measure the errors brought by the change of the coupling strength λ. It is observed that, in the both tasks, the errors is minimized at the common point which coincides with the critical point in r_{var} in Figure 2(c). Note that $\lambda = 3$ indicates where the desynchronization begins. One can confirm that the computational capability of RS attains its maximum at the edge of the synchronization, regardless of the task length($m = 5, 10$ and 15) and types(filtering and predictions).
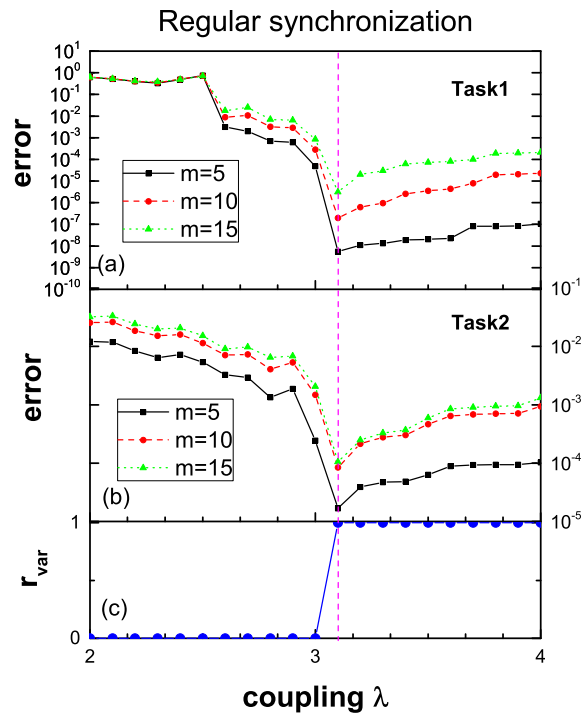
Figure 2: Test error according to the coupling strength in RS. The sudden changes in error in (a) and (b) coincides with the criticality in the variance order parameter in (c).
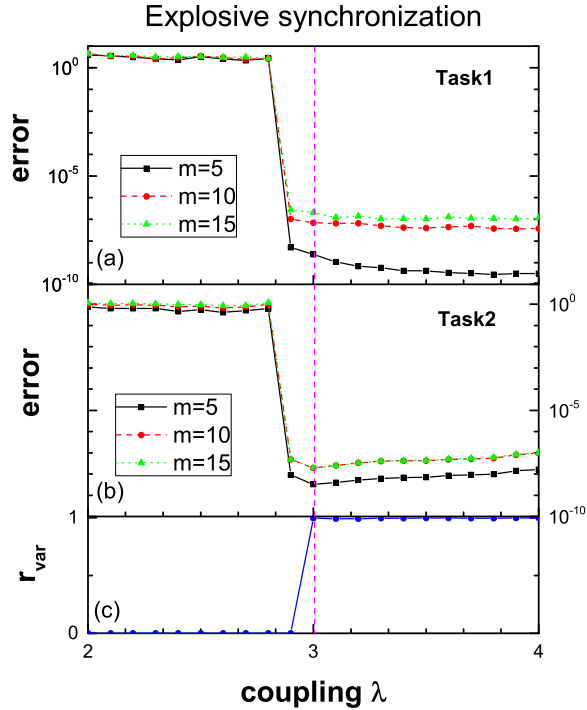
Figure 3: Test error according to the coupling strength in ES. The sudden changes in error in (a) and (b) coincides with the criticality in the variance order parameter in (c).

B. Computing with explosive synchronizations

Having observed the optimized computing ability of RS at criticality, we now turn to the case where the critical transition occurs with the explosive synchronization. We apply ES on a Erdős-Rényi graph with the mean degree $\langle k_i \rangle = 6$. Figure 3 shows that the test errors in the both tasks drop at the common coupling strength, likewise in the case of RS. However, one can see that the accuracy has improved significantly by 10 to 1000 times, compared to those of RS. Another observation is that the error level maintains even for stronger coupling forces beyond the critical point, while it slowly increases in RS in Figure 2.

It is assumed that the computing ability to deal with various input signals in different tasks is closely related to the spectral properties of the system reacting to perturbations. Since individual oscillators in ES hold their own effective frequencies until they turn to have the same effective frequency at the onset of synchronization [28], frequencies of various modes undergo the same criticality. This implies that the system is well prepared for different tasks which involve a wide range of wavelengths. Figure 4 compares the errors of RS and ES according to the task length. While the error of RS sharply increases with the task length, the performance of ES maintains a descent accuracy level in both tasks.
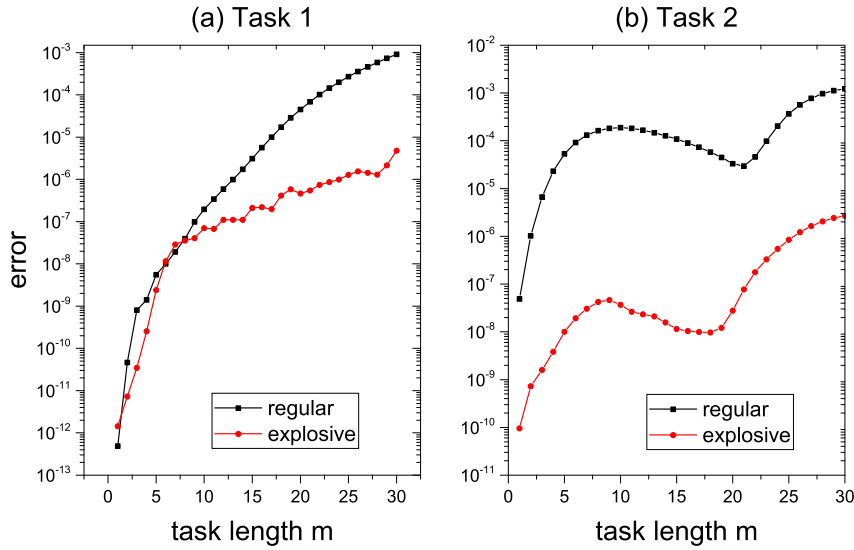
9

Figure 4: Test error according to the task length for RS and ES

In order to investigate the spectral sensitivity of the systems, we additionally test with an input signal of various frequency modes,

$$u(t) = \frac{1}{m} \sum_{i=1}^{m} (a_i \sin(b_i t + c_i) + d_i), \quad a_i, b_i, c_i, d_i \in \mathbb{R}, i = 1, \cdots, m. \tag{8}$$

In Figure 5, the errors of ES grow relatively slower than those of RS as the number of frequency modes m increases.

C. Clear reset in sparse networks

The explosive synchronization can occur on networks with a variety of topological structures, as long as the frequency-coupling relation (2) holds [29]. In this section, we investigate ES in the random networks with various levels of connectivity. Figure 6 illustrates the change of the test errors with respect to the mean degree of Erdős-Rényi graphs. One can see that the performances in two tasks are minimized when the mean degree is at about 6 to 24. If the networks are too sparse, say $\langle k_i \rangle \leq 3$, they are likely to form separate sub-networks, making close cooperation of oscillators impossible. On the contrary, it is noted in Figure 6 that the densely connected oscillators do not work well either. The errors slowly increase with the mean degree as viewed.

These phenomena can be understood in terms of the reset mechanism in computations. Once outputs are generated from transient dynamics induced by inputs, the system should bring its elements to normal condition or the initial state. This is necessary for the system to prepare for next inputs and produce reliable results. In oscillatory networks, a phase-locked state plays a role of this ground state. If the oscillators are densely connected, there are likely excessive ensembles of such ground state. A large number of possible initial states can weaken the capability to
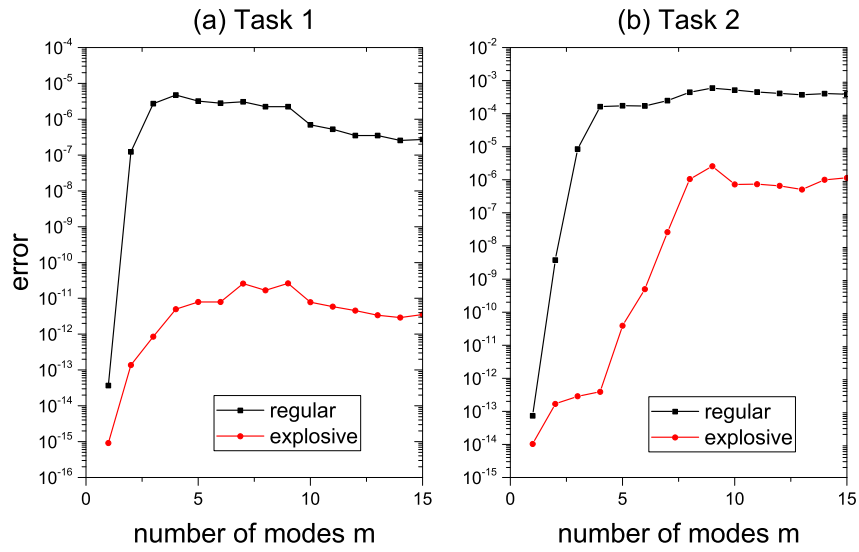
10

Figure 5: Test error according to the number of modes of frequency in the input stream (8) for RS and ES
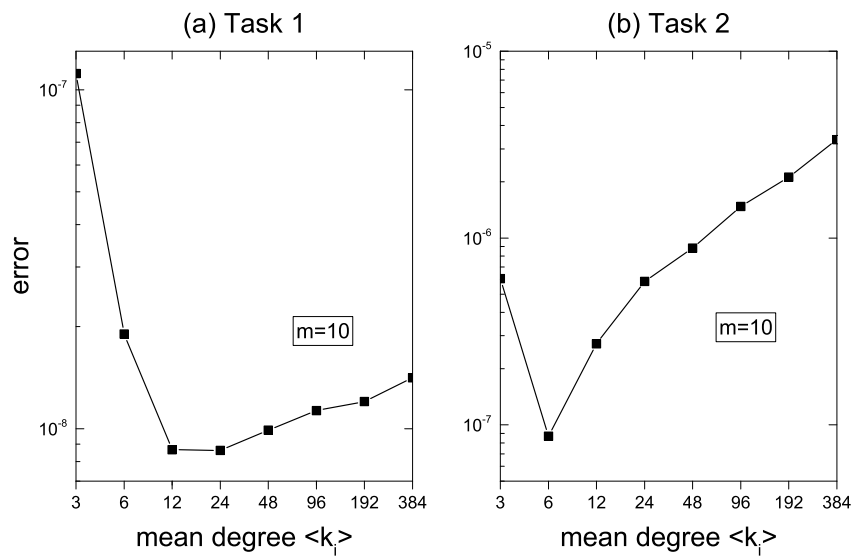

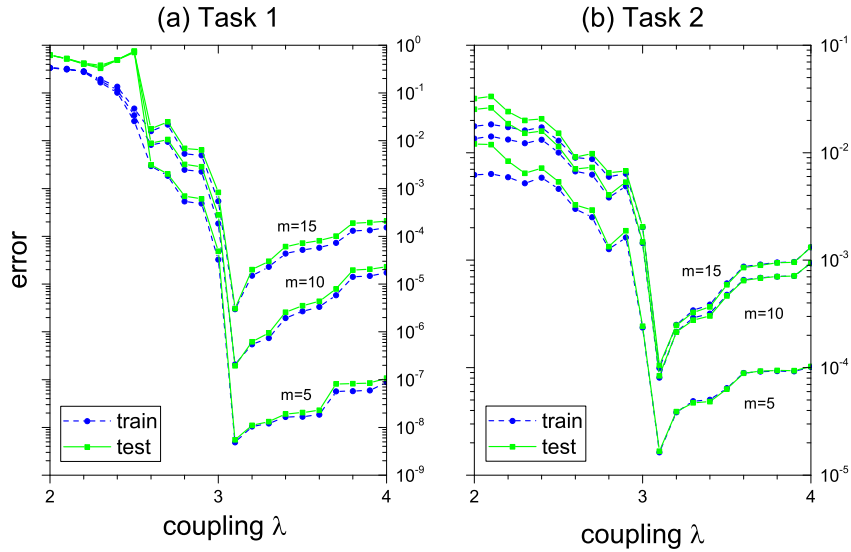Figure 6: Test error according to the mean degree in ES

Figure 7: Training and test error according to the coupling strength in RS. The sudden changes at $\lambda \approx 3$ coincide with the criticality in the variance order parameter.

reproduce consistent results.

D. Phase transition in training error

The order parameter needs to be evaluated first for tuning the systems at the critical regime. However, evaluation of the order parameter could be expensive, even impossible, if access to all oscillators are not feasible. A practical alternative is to measure the training error from the outputs instead of evaluating the order parameters. Figure 7 shows that the training error of RS sharply drops at the same critical point as in Figure 2. That is, one can detect a critical coupling strength from a sudden change in the training error. Note that the training error is kept as high as the test error until the coupling strength reaches a certain level, which implies that RS hardly learns from the training set in a weak coupling regime.

Interestingly, in Figure 8, the more dramatic and exactly opposite situation occurs with ES: the training error keeps low and makes a sharp rise at the critical point. The coupling strength less than the critical value seems to make the reservoir simply reproduce the training data, but fail to process the new data. In other words, the trained model is overfitted with the training data. The reservoir achieves the ability to find the true pattern of the tasks only when the coupling strength is in the regime of the first order criticality. This is notable in that, in reservoir computing, the problem of overfitting is directly related to a property of reservoirs, rather than a way of training them. In contrast to RS, a sudden rise in the training error in ES indicates that the coupling strength reaches a critical level for synchronization.
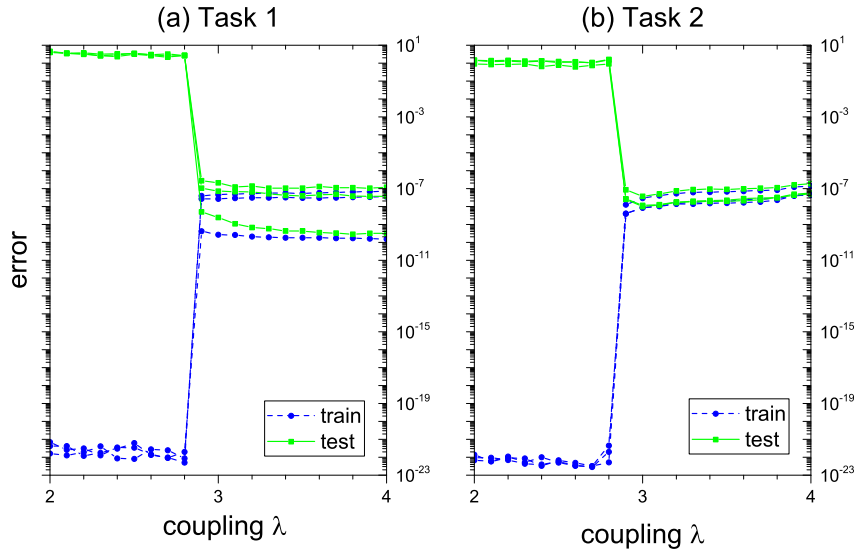
Figure 8: Training and test error according to the coupling strength in ES. The sudden changes at $\lambda \approx 3$ coincide with the criticality in the variance order parameter.

III   Reservoir Computing based on Quenched Chaos

My third section starts.

3.1   Model : Coupled Lorenz Oscillators

A. Reservoir of nonidentical chaotic elements

We consider the reservoir that consists of coupled chaotic oscillators. The reservoir is supposed to suppress chaotic oscillations in its ground state ready for external signals. Recently, the occurrence of an explosive death transition has been found in chaotic oscillator coupled via mean–field diffusion [20]. To extend this result to nonidentical oscillators, we consider a reservoir that consists of N Lorenz systems coupled via a mean–field diffusion as,

$$
\begin{aligned}
\frac{1}{w_i}\frac{dx_i}{dt} &= 10(y_i - x_i) + K(Q\bar{x} - x_i) \\
\frac{1}{w_i}\frac{dy_i}{dt} &= -x_i z_i + \rho x_i - y_i \\
\frac{1}{w_i}\frac{dz_i}{dt} &= x_i y_i - \frac{8}{3}z_i
\end{aligned}
\tag{9}
$$

where, $i = 1, \cdots, N$ is the index of the oscillators. $\bar{x} = \frac{1}{N}\sum_{i=1}^{N} x_i$ is the mean field of the state variable x. The parameter K is the strength of coupling and Q with $0 \leq Q \leq 1$, is the intensity of the mean field. Each single system exactly coincides with the conventional Lorenz system if $K = 0$ with $w_i = 1$. Here we use $Q = 0.7$, following [20]. If the frequencies of nodes are identical, then the systems reverts to the one in [20]. When running the system in (9) as a reservoir, we set the parameters so that the system is posed in a critical regime where the phase transition
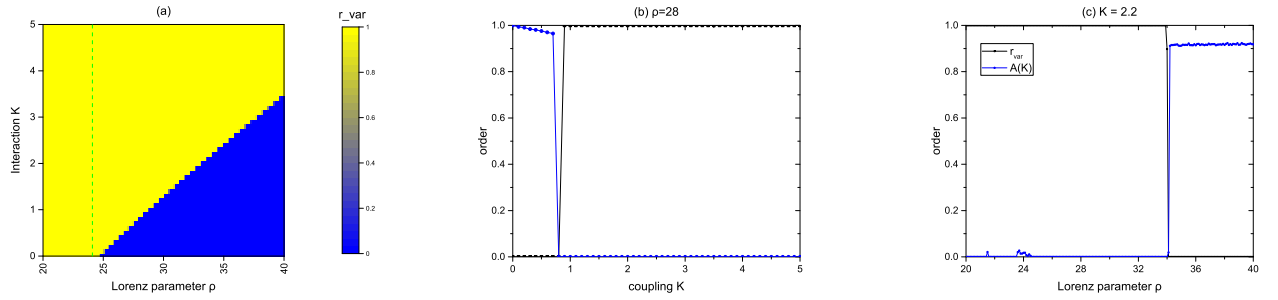
13

Figure 9: Order parameters according to the coupling strength K and lorenz parameter ρ: cross-line at $\rho = 28$ for (b) and $K = 2.2$ for (c), respectively.

occurs. The adjustment of the parameters according to an order parameter will be discussed in Section 3.

B. Creating a criticality by the explosive death

Benefit of using the coupled chaotic systems in (9) as a reservoir is that one can easily create a large criticality by first order phase transition in the system. Across a critical point of the coupling force, the compound oscillatory motions of the system, collapse into an equilibrium point. This fixed equilibrium state near a critical point is used as the ground state for reservoir computing, where the system always returns to after every computation, erasing unnecessary information from previous evaluations and preparing for the next inputs.

To look for a possible phase transition in (9), we take order parameter r_{var} in terms of the variation of amplitudes, as defined in the previous section (3).

If the frequencies of nodes in (9) are identical, then the system exhibits explosive death, the discontinuous transition from the oscillatory state to the completely quenched state [20]. Indeed, (9) with nonidentical natural frequencies still exhibits the same phenomena. Figure 9(a) is the graph of the order parameter r_{var} in the ρ-K parameter space. N=100 of Lorenz systems are coupled via mean-field diffusion with Q=0.7. The natural frequencies follow the uniform distribution in $[1, 1.3]$. And the dynamical states of system was obtained by backward continuation starting at large enough K and then lowering gradually [20]. The order parameter r_{var} was averaged between t=[3900, 4000]. The dotted line separates non-chaotic part(left) and chaotic part(right),where we are interested in, when coupling K is 0.

To be more certain, we propose the widely used order parameter for chaotic oscillators $A(K)$, which is the normalized average amplitude [20].

$$A(K) = \frac{a(K)}{a(0)}, \quad a(K) = \frac{\sum_{i=1}^{N}(\langle x_{i,max}\rangle_t - \langle x_{i,min}\rangle_t)}{N} \tag{10}$$

The graph in Figure 9.(b) and (c) indicate cross-sectional figures in K and ρ directions, respectively. It is shown that both of the order parameters exhibit extremely abrupt jump at
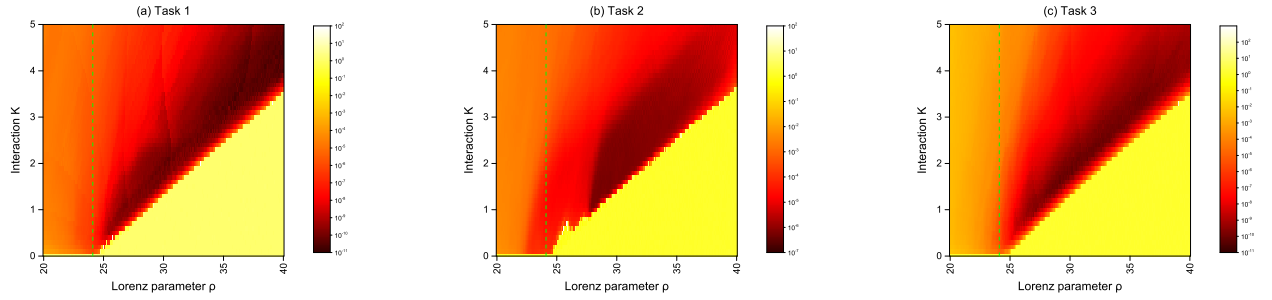
14

Figure 10: Test error according to the lorenz system parameter ρ and coupling K.
(a): rossler y-data reconstruction, (b): chua y-data reconstruction and (c): mackey-glass past 20 input summation.

the same transition line across the plane. The line clearly separates the region of the amplitude death from incoherent states, indicating where the first order transition occurs with respect to K.

3.2 Numerical Tests

In the following numerical examples to test the learning ability of the oscillator networks, we use the $(10, 0.1)-$type readout : The output function f_{out} at t is obtained from 10 previous sampled values of the oscillator frequencies $x_i'(t), \cdots, x_i'(t - 0.9)$ through the (4).

We set up two types of tasks, inferring missing variables and deriving past inputs (7), both of which require the presence of long-term memory for proper execution. The first two tasks are to reconstruct values of hidden variables of the systems from observation of a single variable. For example, suppose a temporal data $(x(t), y(t), z(t))$ is generated from an unknown system. The reservoir is trained to infer $y(t)$ and $z(t)$ as the output from the input $x(t)$. This implies that RC implicitly learns a structure of the system that generates the corresponding data. We use two chaotic systems to generate the data, Rossler system, and Chua's circuit.

In each task, the continuous input signal $u(t)$ and the target signal $v(t)$ are generated for $t \in [0, 6000]$. To sure that the system is positioned in the reliable ground state, skipped first 1000 time steps. The training process is applied to match f_{out} to $v(t)$ over the 4,000 discrete time steps, $t = 1001, 1002, \cdots, 5000$. That is, the readout weights $w_{i,j}^l$ in (4) are determined to minimize the relative error (6). Then we measure the performance using the remaining part of the signal for $t \in (5000, 6000]$: the relative error (6) between f_{out} to $v(t)$ is evaluated over 1,000 discrete sampled time steps.

Figure 10 depicts the errors in task 1 to 3 with respect the parameters ρ and K. In all the tasks, minimum error occurs along the same line below left. One can see that the line forms a clear border across which the error jumps from the low error regime (red) to high error regime (yellow). It should be noted that the line is indeed the aligned critical points as in Figure 10 where the explosive death of the nodes occurs. This assures that the computational

15

performance of the reservoirs is maximized near the first order phase transition. The dotted line quite obviously separates(or seems to separate) the tendency of errors as Figure 10.

IV Comparison : information processing capacity

In the previous section [31], a reservoir that consists of regular phase oscillators(ES) was presented as

$$\theta'_i = \omega_i + \frac{\lambda|w_i|}{k_i} \sum_{j=1}^{N} A_{ij} \sin(\theta_j - \theta_i), \quad i = 1, \cdots, N, \tag{11}$$

where λ is the coupling strength of oscillators and A_{ij} the entry of the adjacency matrix of the network. Here we take $A_{ij} = 1$ if $i \neq j$, otherwise 0. The reservoir shows great performance improvement across a critical point for synchronization. Effect of criticality is larger when the corresponding criticality is of the first order (discontinuous) phase transition, rather than the second order (continuous) one. In Section 3, we observed that the reservoir of coupled chaotic elements(QC) also achieves best performance at the first order phase transition(explosive death). This section tries to compare the performance of the above two critical reservoirs, regular and chaotic ones, when both are being poised at the first order phase transition.
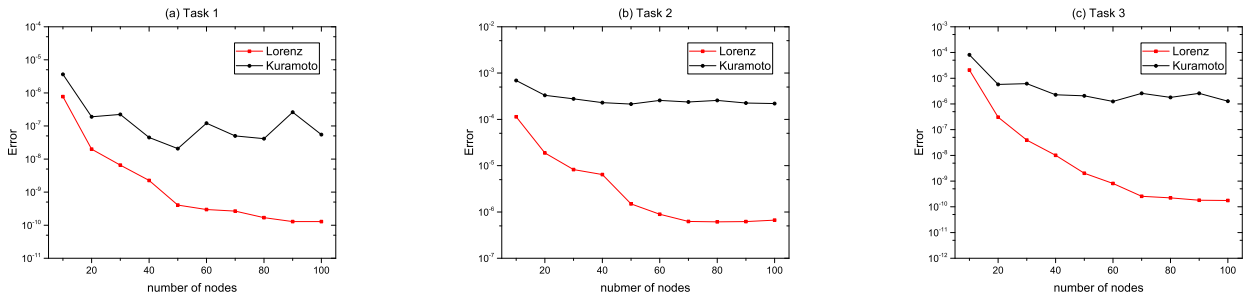

Figure 11: Test errors of QC and ES with respect to number of nodes.

Figure 11 depicts the errors of QC and ES with task 1 to 3, respectively. In all of three tasks, QC works much better than ES. Moreover, as the number of nodes increases, the difference becomes clearer. It seems that the computaion ability of QC continuouly increases continuosly while ES only increases till about 40 nodes. One of possible explanations on superiority of the chaotic reservoir is that the computing capability of critical reservoirs may depend on the collapsed dimension of attractors of reservoirs across the critical point. That is, the effect of criticality on computing performance may be related to how much reduction occurs in the dimension of the synchronization manifold at the phase transition. One can guess that the collapsed dimension of (9) at the explosive death is much greater than that of (11), from the fact that an attractor of a single Lorenz system has a greater Hausedorff dimension($\sim$2.06), compared to one dimensional attractor of a phase oscillator. However, unfortunately, computing the dimension of an attractor of a large coupled chaotic system is extremely time-consuming and not practical.

For more practical caparison, we adopt the information processing capacity which has been introduced in [27] to compute the capacity of input driven dynamical systems. We especially

compare the total capacity C_{TOT}, the summation of $C_T[X, y_l]$ $\forall y_l \in Y_L$ for some dynamical system X, where Y_L tends towards a complete orthogonal set of functions in the fading memory Hilbert space. The capacity, equation (5) in [27], $C_T[X, z]$ measures how successful the dynamical system X is at computing z. Here, we use the dynamical system QC and ES for X. The most principal advantage of C_{TOT} is the property, bounded by the size of readout, which provide convenient way to compare given systems. To avoid numerical problems, $C_T^\epsilon(X, \{d_i\})$ in (12) is substituted for $C_T[X, d_i]$. We refer the reader to [27] for more details on the information capacity of dynamical system.

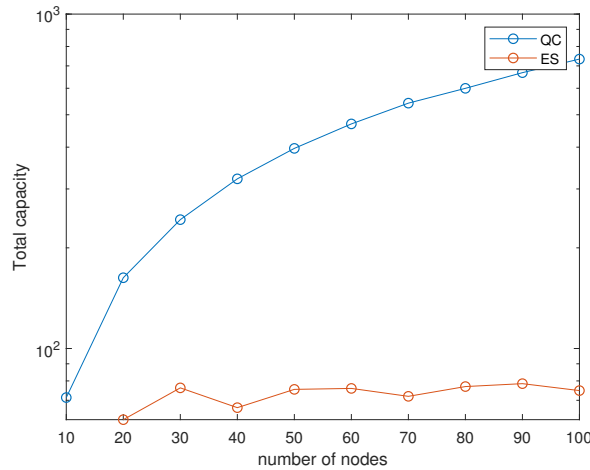$$C_{TOT}[C] = \sum_{\{d_i\}} C_T^\epsilon(X, \{d_i\}) \tag{12}$$

Figure 12: Total information capacity C_{TOT} with respect to number of oscillators. Capacity is bounded by 10 times to the number of nodes for our RC. We took input from unifrom distribution over the interval [-1,1] and finite products of normalized Legendre polynomials for y_l. The total measured capacity was derived according to the degree $\sum_{i=1}^{5} d_i$.

Figure 4 compares C_{TOT} of regular and chaotic reservoirs. We can check that the capacity of QC continuouly increases, but the capacity of ES doesn't increases after about 30 nodes which agrees with the results of the numerical tasks in Figure 11. So we expect that C_{TOT} can be an reliable measure for the capacity of coupled oscillators for computation.

V   Conclusion

With a low coupling strength, oscillators are not able to form a consistent initial state from where valid computation can start. On the contrary, an excessive coupling strength suppresses dynamics perturbed by external stimuli too quickly, preventing it from working for efficient computation. Simulations showed that networks of phase oscillators maximize their dynamic range of information processing when configured on the edge of the synchronization. They can provide a general framework for neuromorphic computing in that their synchronoy can be easily controlled by the coupling strength. Especially in the explosive synchronization, in a critical parameter regime where every mode of frequencies undergoes simultaneous synchronization, the computing performance is greatly improved compared to that of the regular synchronization.

To find the critical coupling strength, we used the variance order parameter that clearly indicates the onset of phase-locking by discontinuous jump in either regular or explosive synchronization. However, since evaluation of the variance order parameter needs a long-time access to the entire network, measuring it can be impractical, if not impossible. We showed that tracking the training error can replace the order parameter: one can increase the coupling strength until there appears a sudden change (up/down) in the training error. Since evaluating the training error is a part of every learning process, we can locate the critical coupling strength without additional cost.

In section 3 and 4, we showed that the coupled chaotic systems in the regime of quenched chaos(amplitude death) can be used for efficient reservoir computing. As the reservoir of the coupled phase oscillators at explosive synchronization, the chaotic reservoirs utilize a criticality at the first order (discontinuous) phase transition to create a ground state for computation. It notices in several computing tasks that the chaotic reservoirs excel the regular reservoirs, which is also confirmed from comparing their information capacity.

The results imply that using chaotic nodes is more beneficial in constructing reservoirs. This finding is important in several aspects. First of all, chaos is widely observed in neuronal systems, both experimentally and theoretically [32]. We confirmed that such ubiquity of chaos can be justified from the perspective of computing. That is, as long as it is properly quenched in the critical regime, chaos is an goal worth pursuing rather than an undesirable state to be avoided. Chaos computing is the paradigm that exploits the controlled richness of nonlinear dynamics to do flexible computations. This work shows another theoretical direction of chaos computing different from the approach using chaotic elements to emulate different logic gates [33,34]. Basic understanding of a role of criticality in regular and chaotic reservoirs can be expected to shed light on how information is processed in quenched coupled nonlinear systems, potentially leading to proposition of a broad range of reservoirs.

References

[1] G. Tanaka, T. Yamane, J. B. Héroux, R. Nakane, N. Kanazawa, S. Takeda, H. Numata, D. Nakano, and A. Hirose, "Recent advances in physical reservoir computing: a review," *Neural Networks*, 2019.

[2] R. Legenstein and W. Maass, "Edge of chaos and prediction of computational performance for neural circuit models," *Neural Networks*, vol. 20, no. 3, pp. 323–334, 2007.

[3] C. G. Langton, "Computation at the edge of chaos: phase transitions and emergent computation," *Physica D: Nonlinear Phenomena*, vol. 42, no. 1-3, pp. 12–37, 1990.

[4] J. M. Beggs and D. Plenz, "Neuronal avalanches in neocortical circuits," *Journal of neuroscience*, vol. 23, no. 35, pp. 11 167–11 177, 2003.

[5] J. M. Beggs and N. Timme, "Being critical of criticality in the brain," *Frontiers in physiology*, vol. 3, p. 163, 2012.

[6] M. Botcharova, S. F. Farmer, and L. Berthouze, "Markers of criticality in phase synchronization," *Frontiers in systems neuroscience*, vol. 8, p. 176, 2014.

[7] B. Del Papa, V. Priesemann, and J. Triesch, "Criticality meets learning: Criticality signatures in a self-organizing recurrent neural network," *PloS one*, vol. 12, no. 5, p. e0178683, 2017.

[8] H. Jaeger and H. Haas, "Harnessing nonlinearity: Predicting chaotic systems and saving energy in wireless communication," *science*, vol. 304, no. 5667, pp. 78–80, 2004.

[9] J. F. Miller and K. Downing, "Evolution in materio: Looking beyond the silicon box," in *Proceedings 2002 NASA/DoD Conference on Evolvable Hardware*. IEEE, 2002, pp. 167–176.

[10] M. A. Munoz, "Colloquium: Criticality and dynamical scaling in living systems," *Reviews of Modern Physics*, vol. 90, no. 3, p. 031001, 2018.

[11] M. F. Crowley and I. R. Epstein, "Experimental and theoretical studies of a coupled chemical oscillator: phase death, multistability and in-phase and out-of-phase entrainment," *The Journal of Physical Chemistry*, vol. 93, no. 6, pp. 2496–2502, 1989.

[12] M. Dolnik and I. R. Epstein, "Coupled chaotic chemical oscillators," *Physical Review E*, vol. 54, no. 4, p. 3361, 1996.

[13] G. Ermentrout and N. Kopell, "Oscillator death in systems of coupled neural oscillators," *SIAM Journal on Applied Mathematics*, vol. 50, no. 1, pp. 125–146, 1990.

[14] I. Ozden, S. Venkataramani, M. Long, B. Connors, and A. Nurmikko, "Strong coupling of nonlinear electronic and biological oscillators: reaching the "amplitude death" regime," *Physical review letters*, vol. 93, no. 15, p. 158102, 2004.

[15] R. Herrero, M. Figueras, J. Rius, F. Pi, and G. Orriols, "Experimental observation of the amplitude death effect in two coupled nonlinear oscillators," *Physical review letters*, vol. 84, no. 23, p. 5312, 2000.

[16] M.-D. Wei and J.-C. Lun, "Amplitude death in coupled chaotic solid-state lasers with cavity-configuration-dependent instabilities," *Applied Physics Letters*, vol. 91, no. 6, p. 061121, 2007.

[17] V. Resmi, G. Ambika, and R. Amritkar, "General mechanism for amplitude death in coupled systems," *Physical Review E*, vol. 84, no. 4, p. 046212, 2011.

[18] N. Zhao, Z. Sun, X. Yang, and W. Xu, "Explosive death of conjugate coupled van der pol oscillators on networks," *Physical Review E*, vol. 97, no. 6, p. 062203, 2018.

[19] U. K. Verma, A. Sharma, N. K. Kamal, and M. D. Shrimali, "First order transition to oscillation death through an environment," *Physics Letters A*, vol. 382, no. 32, pp. 2122–2126, 2018.

[20] U. K. Verma, A. Sharma, N. K. Kamal, J. Kurths, and M. D. Shrimali, "Explosive death induced by mean–field diffusion in identical oscillators," *Scientific reports*, vol. 7, no. 1, p. 7936, 2017.

[21] I. Leyva, R. Sevilla-Escoboza, J. Buldú, I. Sendina-Nadal, J. Gómez-Gardeñes, A. Arenas, Y. Moreno, S. Gómez, R. Jaimes-Reátegui, and S. Boccaletti, "Explosive first-order transition to synchrony in networked chaotic oscillators," *Physical review letters*, vol. 108, no. 16, p. 168702, 2012.

[22] A. Babloyantz and C. Lourenço, "Computation with chaos: A paradigm for cortical activity," *Proceedings of the National Academy of Sciences*, vol. 91, no. 19, pp. 9027–9031, 1994.

[23] C. Lourenço, "Attention-locked computation with chaotic neural nets," *International Journal of Bifurcation and Chaos*, vol. 14, no. 02, pp. 737–760, 2004.

[24] ——, "Dynamical reservoir properties as network effects." in *ESANN*, 2006, pp. 503–508.

[25] ——, "Dynamical computation reservoir emerging within a biological model network," *Neurocomputing*, vol. 70, no. 7-9, pp. 1177–1185, 2007.

[26] ——, "Structured reservoir computing with spatiotemporal chaotic attractors." in *ESANN*, 2007, pp. 501–506.

[27] J. Dambre, D. Verstraeten, B. Schrauwen, and S. Massar, "Information processing capacity of dynamical systems," *Scientific reports*, vol. 2, p. 514, 2012.

[28] J. Gómez-Gardenes, S. Gómez, A. Arenas, and Y. Moreno, "Explosive synchronization transitions in scale-free networks," *Physical review letters*, vol. 106, no. 12, p. 128701, 2011.

[29] X. Zhang, X. Hu, J. Kurths, and Z. Liu, "Explosive synchronization in a general complex network," *Physical Review E*, vol. 88, no. 1, p. 010802, 2013.

[30] M. Casdagli, "Nonlinear prediction of chaotic time series," *Physica D: Nonlinear Phenomena*, vol. 35, no. 3, pp. 335–356, 1989.

[31] J. Choi and P. Kim, "Critical neuromorphic computing based on explosive synchronization," *Chaos: An Interdisciplinary Journal of Nonlinear Science*, vol. 29, no. 4, p. 043110, 2019.

[32] K. Aihara, "Chaotic oscillations and bifurcations in squid giant axons," *Chaos*, pp. 257–269, 1986.

[33] S. Sinha and W. L. Ditto, "Dynamics based computation," *physical review Letters*, vol. 81, no. 10, p. 2156, 1998.

[34] ——, "Computing with distributed chaos," *Physical Review E*, vol. 60, no. 1, p. 363, 1999.

Acknowledgements

First of all, I would like to thank my advisor Pilwon Kim, I had a lot of help with proceeding my research and ideas, but most of all, it was really helpful of him when I had my question about whether to continue studying. Thanks to my family and colleagues who helped me to concentrate on study and research, I was able to overcome many procedures without getting tired easily. And I would like to express my gratitude to myself for doing the best I can during last two years.